Origin of negative thermal expansion in strongly correlated *f*-electron systems

Junwon Kim [1] J.-S. Kang [2] Chang-Jong Kang [3] and B. I. Min [1,*]

[1]*Department of Physics, Pohang University of Science and Technology, Pohang 37673, Korea*
[2]*Department of Physics, The Catholic University of Korea, Bucheon 14662, Korea*
[3]*Department of Physics, Chungnam National University, Daejeon 34134, Korea*

We have investigated the origin of the negative-thermal-expansion (NTE) phenomena observed in various strongly correlated *f*-electron systems, including Ce, Sm, and Yb rare-earth compounds and actinide element Pu. We have thoroughly surveyed existing nonmagnetic *f*-electron NTE materials and identified that the temperature (*T*)-induced valence transition plays an essential role in realizing the NTE in Sm- and Yb-based mixed-valence (MV) systems. We have discussed the contrasting thermal-expansion behaviors between (Sm, Yb)-based MV systems and their electron-hole symmetric counterparts (Ce, Eu)-based MV systems that exhibit positive-thermal-expansion (PTE) phenomena. We have also clarified the origin of intriguing thermal expansion behavior of Pu, which, upon cooling, reveals not only the NTE, but also the strong PTE. Finally, we have predicted the possible existence of an additional NTE feature in topological-Kondo-insulator (TKI) candidates of SmB_6, g-SmS, and YbB_{12} in the low-*T* regime where the TKI nature is expected to emerge.

I. INTRODUCTION

It is commonly recognized that the volume of a solid system increases with increasing temperature (*T*). This phenomenon of thermal expansion is well known to originate from the inherent anharmonic ion-ion interaction in solids [see Fig. 6(a) in the Appendix]. But there are some systems that exhibit abnormal thermal contraction with increasing *T*, which are dubbed negative-thermal-expansion (NTE) systems [1–10]. In fact, NTE systems are ubiquitous, not only in weakly correlated *s*- and *p*-electron solids, but also in strongly correlated *d*- and *f*-electron solids. For example, Si [11], Ge [11], Te [12], and ZrW_2O_8 [13] belong to the former, whereas the famous Invar system of the $Fe_{0.65}Ni_{0.35}$ alloy [14] belongs to the latter.

Note that the thermal-expansion coefficient $\alpha_V [\equiv \frac{1}{V}(\frac{\partial V}{\partial T})_P]$ is proportional to the Grüneisen parameter γ_G ($\alpha_V = \gamma_G c_V / B$), where V, P, c_V, and B are the volume, pressure, specific-heat per volume, and bulk modulus of a system, respectively [4,5]. Hence, negative γ_G would bring about negative α_V. In fact, γ_G is determined not only by phonon contributions (γ_G^p), but also by electron contributions (γ_G^e), and so α_V had better be expressed more explicitly as [$\alpha_V = (\gamma_G^p c_V^p + \gamma_G^e c_V^e)/B$] [2]. In general, the NTE in weakly correlated electron systems has the phonon origin. Namely, negative γ_G results from the behavior of a specific transverse-phonon mode or rigid-unit mode [Fig. 6(b) in the Appendix] under pressure ($\gamma_G^p = -\frac{\partial \ln \hbar\omega_p}{\partial \ln V}$).

In contrast, the NTE in strongly correlated electron systems has the electron origin for which negative γ_G results from the predominant pressure-induced behavior of a characteristic electronic-energy scale (E_c) ($\gamma_G^e = -\frac{\partial \ln E_c}{\partial \ln V}$), such as the energy difference between relevant states, crystal-field splitting, Kondo temperature, and so on.

For example, the NTE in Invar systems has been explained by taking into account the energy difference between the magnetic (high-spin) ground state having the larger volume and the nonmagnetic (low-spin) metastable state having the smaller volume [9,15–17], as provided in Fig. 1. That is, the electronic peculiarity is to be realized in the lattice anomaly due to close interplay between electron and lattice degrees of freedom. For Invar, the magnetovolume effect plays such a role [2,5,8,10].

For strongly correlated *f*-electron rare-earth (RE) and actinide systems, there are magnetic as well as nonmagnetic NTE systems. The NTE mechanism for magnetic *f*-electron systems is basically the same as that for Invar. For nonmagnetic *f*-electron systems, however, the understanding of the NTE mechanism is still far from complete, which motivates the present paper

Table I provides various nonmagnetic (and nonsuperconducting) *f*-electron NTE systems collected from literature, which include heavy-fermion, mixed-valence (MV), and Kondo systems of Ce, Sm, and Yb compounds as well as actinide Pu. Accordingly, the NTE mechanism for these systems is expected to be closely related to their relevant *f*-electron physics. The Sm and Yb-based NTE systems listed in Table I are mostly MV systems, but Ce-based NTE systems in Table I are rather categorized as heavy-fermion systems. Note that typical Ce-based MV systems, $CePd_3$ and $CeSn_3$, do not exhibit the NTE feature [45]. In this respect, the NTE mechanism for Ce-based NTE systems in Table I is thought to be different from those for Sm- and Yb-based NTE systems [20,46]. One more notable thing in Table I is that, among 5*f*-electron actinide systems, the fcc phase of Pu (*δ*-Pu), exhibits the NTE feature [47].

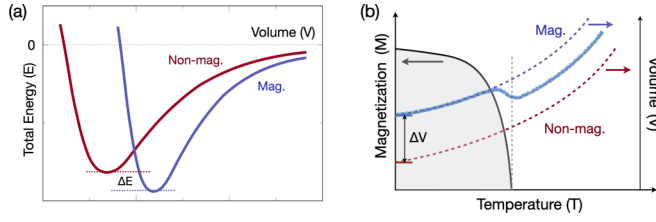*Corresponding author: bimin@postech.ac.kr

FIG. 1. Two-state model for the NTE of Invar. (a) Total energies vs volume for the magnetic (Mag) or high-spin ground state and the nonmagnetic (Non-mag) or low-spin metastable state at $T = 0$. (b) Magnetization M and (c) volume changes as a function of T. Without the electronic contribution, the volume of each state will expand normally upon heating as depicted by dotted lines. The state at high T corresponds to a mixed state of Mag and Non-mag [16]. Note that $\frac{\partial V}{\partial T} = \frac{\partial V}{\partial M} \frac{\partial M}{\partial T}$. Then, $\frac{\partial V}{\partial M} > 0$ from (a) and $\frac{\partial M}{\partial T} < 0$ below T_c from (b) yields the NTE ($\frac{\partial V}{\partial T} < 0$). For real magnetic materials, depending on the sizes of ΔE and ΔV, not only the NTE, but also the zero or positive thermal expansion is manifested.

In this paper, we have investigated the NTE mechanisms observed in the f-electron MV systems. In the RE systems, the different valence states have very different volumes, and so the valence transitions in RE MV compounds are accompanied by large volume changes. In consequence, the RE MV compounds would display anomalous thermal expansion phenomena.

We address here the following issues. First, we have discussed the contrasting thermal-expansion behaviors between (Sm, Yb)-based MV systems that exhibit NTE and (Ce, Eu)-based MV systems that exhibit positive-thermal-expansion (PTE). For the Ce element, we have examined the effect of the f-electron coherence, which plays an essential role in the γ-α phase transition and the manifestation of the strong PTE. Then, we have clarified the origin of intriguing thermal expansion behavior of Pu, which, upon cooling, reveals not only the NTE, but also the strong PTE [48]. Finally, for SmB$_6$, g-SmS, and YbB$_{12}$, which were recently proposed to be topological Kondo insulators (TKIs) [49–52], we have predicted, based on the thermodynamic relation, the possible existence of an additional NTE feature in the low-T regime.

II. NTE IN (SM, YB)-BASED VS PTE IN (CE, EU)-BASED MV SYSTEMS

In Fig. 2 are plotted the thermal expansion data of typical f-electron MV systems and the Ce element. As shown in Figs. 2(a)–2(d), Sm compounds (SmB$_6$, SmS) and Yb compounds (YbCuAu, YbB$_{12}$) reveal the NTE feature characterized by the volume minimum at a certain T, which is

considered to be corresponding to the valence-transition temperature, T_{VT} [31,42,54]. It is well known that the volume of an f-electron RE system depends sensitively on its valence state. Hence, if the valence state varies with T in the MV systems, the volume also changes with T,

$$\frac{\partial V}{\partial T} = \frac{\partial V}{\partial n_f} \frac{\partial n_f}{\partial T}, \qquad (1)$$

where n_f is the occupation number of f electrons. This kind of dynamical valence fluctuation arising from the T-induced change in the electronic structure is characteristic of strongly correlated electron systems, which has been described by employing the Kondo or Anderson model Hamiltonian [55].

For Sm- and Yb-based MV compounds, the valence transition occurs from the near-trivalent state (f^5, f^{13}) having the smaller volume to near-divalent MV state (f^6, f^{14}) having the larger volume upon cooling, and so the volume starts to increase below T_{VT} ($\frac{\partial V}{\partial T} > 0$) because $\frac{\partial V}{\partial n_f} > 0$ and $\frac{\partial n_f}{\partial T} < 0$ for $T < T_{VT}$. This is why the volume minimum is located near T_{VT}. It is seen that T_{VT}'s are roughly 150, 80, 75, and 70 K for SmB$_6$, g-SmS, YbCuAu, and YbB$_{12}$, respectively.

Interestingly, this behavior in (Sm, Yb)-based MV systems contrasts with that in (Ce, Eu)-based MV systems that exhibit just monotonic volume reductions upon cooling, producing the PTE. It happens because, in Ce-based MV (e.g., CePd$_3$ and CeSn$_3$ [45]) and Eu-based MV (e.g., EuPd$_2$Si$_2$ [56–58]) systems, which are electron-hole symmetric counterparts of Sm and Yb systems [Fig. 2(h)], the valence transitions occur, upon cooling, from the near-f^1 and near-f^7 configurations having larger volumes to the near-f^0 and near-f^6 MV configurations having smaller volumes. As a consequence, $\frac{\partial V}{\partial n_f} > 0$ and $\frac{\partial n_f}{\partial T} > 0$, and so the volume decreases ($\frac{\partial V}{\partial T} > 0$) below T_{VT} as shown in Fig. 2(g) for EuPd$_2$Si$_2$ ($T_{VT} \approx 160$ K). Similarly, CeSn$_3$ exhibits the PTE feature ($T_{VT} \approx 260$ K) as shown in Fig. 7 in the Appendix [45,59].

Figures 3(a)–3(f) describe schematically the different thermal-expansion behaviors between the Sm compound of g-SmS and the Eu compound of EuPd$_2$Si$_2$. For g-SmS, the ground state is the MV state ($n_f \approx 5.4$) having a larger volume than the high-T near-trivalent (III) state as depicted in Fig. 3(a), and n_f decreases from the MV state to the near-trivalent state upon heating [Fig. 3(b)]. Then, the NTE mechanism for g-SmS can be explained by the two-state Weiss model employed for Invar as sketched in Fig. 3(c). For g-SmS, the volume minimum was observed near $T_{VT} \approx 80$ K [27]. The NTE phenomena for most (Sm, Yb)-based MV systems can be understood in the same way.

TABLE I. Representative nonmagnetic f-electron NTE systems.

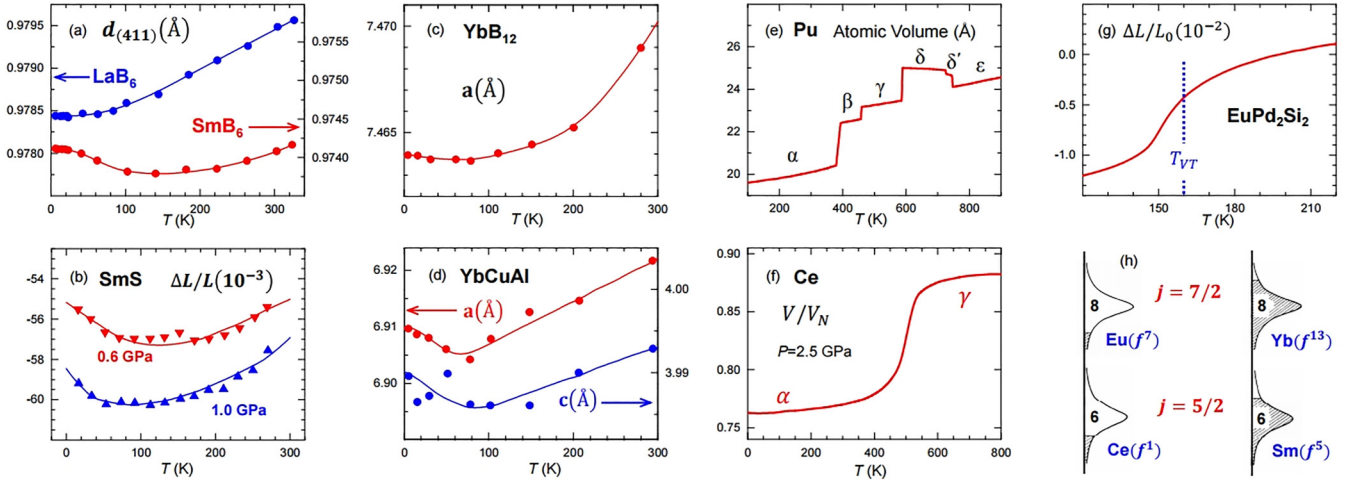| Base	NTE systems
Ce	Ce(La)Al$_2$ [18], CeAl$_3$ [19], CeB$_4$ [20], Ce(La)B$_6$ [21], and CeInCu$_2$ [22]
Sm	SmB$_6$ [23–25], Sm$_{2.75}$C$_{60}$ [26], g-SmS [27,28], and Sm(Y)S [29–31]
Yb	YbAl$_3$ [32], YbB$_{12}$ [33], YbB$_{50}$ [34], Yb$_{2.75}$C$_{60}$ [35], YbCuAl [36–38], YbCu$_2$Si$_2$ [39], YbCu$_4$Ag [40], YbInAu$_2$ [41], YbInCu$_4$ [42], YbInPd [41], YbNi$_2$Ge$_2$ [41], YbPd [43], and YbT_2Zn$_{20}$ ($T =$ Co, Rh, Ir) [44]
Pu	δ-Pu [47,48]

FIG. 2. Thermal expansion data of f-electron NTE systems: (a) SmB_6 (with LaB_6 for comparison), (b) g-SmS, (c) YbB_{12}, (d) YbCuAl, and (e) actinide element Pu. PTE data of (f) Ce element and (g) $EuPd_2Si_2$ ($T_{VT} \approx 160$ K) are also shown for comparison. (h) Typical electronic configurations of Ce (f^1) and Sm (f^5) compounds occupying $j = 5/2$ f states, and Eu (f^7) and Yb (f^{13}) compounds occupying $j = 7/2$ f states. There is an electron-hole symmetry between (Ce, Eu) and (Sm, Yb). Data adapted from Refs. [25,27,33,36,48,53,58] for (a)–(g), respectively.

On the other hand, for $EuPd_2Si_2$, the ground state is the MV state ($n_f \approx 6.2$) having a smaller volume than the high-T near-divalent (II) state ($n_f \approx 7$) as depicted in Fig. 3(d). Upon heating, n_f increases from the MV state to the near-divalent state [Fig. 3(e)]. Then, the PTE observed in $EuPd_2Si_2$ can also be explained by employing the two-state Weiss model as sketched in Fig. 3(f). The PTE phenomena observed for most (Ce, Eu)-based MV systems can be understood in the same way. It is, thus, inferred from Fig. 3 that, for the MV systems, the NTE would be realized when their excited states have smaller volumes [Fig. 3(a)], whereas the PTE would be realized when their excited states have larger volumes [Fig. 3(d)].

III. PTE IN CE

For the Ce element, there is an additional f-electron bonding effect below the coherent temperature T_{coh} at which f electrons become coherent to form delocalized f bands ($T_{coh} \approx 129$ K for α-Ce at the ambient pressure) [60,61]. This effect brings about the volume collapse for Ce, upon cooling, as shown in Fig. 2(f).

Figures 4(a)–4(c) describe schematically the thermal-expansion behavior in the Ce element. For Ce, localized $4f$ electrons in γ-Ce, that is, a stable phase at room T become delocalized via coherent f-band formation upon cooling, resulting in the ground-state phase of α-Ce having the smaller volume as depicted in Fig. 4(a). The valence state of Ce does
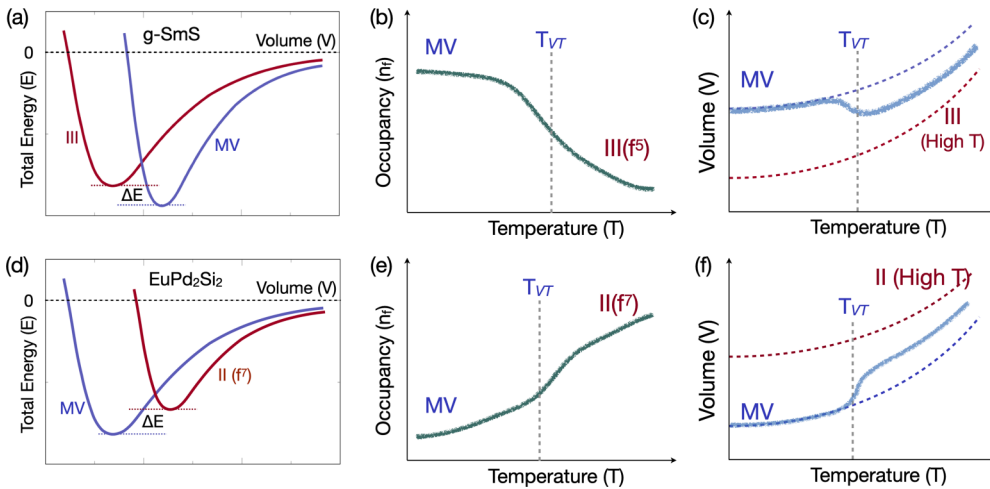

FIG. 3. Total energies vs volume (V) for different electronic states, the valence state [occupancy (n_f)], and the volume changes as a function of T for g-SmS and $EuPd_2Si_2$. (a)–(c) For g-SmS, $\frac{\partial V}{\partial n_f} > 0$, and $\frac{\partial n_f}{\partial T} < 0$, and so $\frac{\partial V}{\partial T} = \frac{\partial V}{\partial n_f} \frac{\partial n_f}{\partial T} < 0$ below T_{VT} (III: Near-trivalent state). (d)–(f) For $EuPd_2Si_2$, $\frac{\partial V}{\partial n_f} > 0$ and $\frac{\partial n_f}{\partial T} > 0$, and so $\frac{\partial V}{\partial T} = \frac{\partial V}{\partial n_f} \frac{\partial n_f}{\partial T} > 0$ below T_{VT} (II: Near-trivalent state). Dotted lines in (c) and (f) represent normal thermal expansions of $V(T)$ without the electronic contributions.
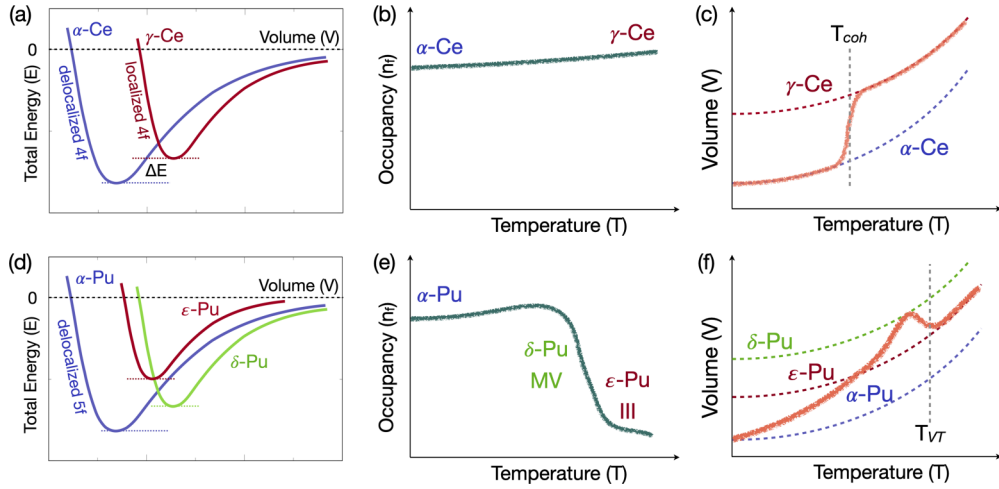
FIG. 4. Schematics of total energies vs volume (V) for different electronic states, the valence state [occupancy (n_f)], and the volume changes as a function of T for Ce and Pu. (a)–(c) For Ce, strong PTE coefficient originates from the coherent f-band formation in the ground state of α-Ce, upon cooling, from the metastable state of γ-Ce. (d)–(f) For Pu, total energies vs volume for typical three-different phases, α-, δ-, and ϵ-Pu. We have now three states. Upon cooling from high T, the valence transition occurs first from near-trivalent ϵ-Pu to MV δ-Pu, and then the coherent $5f$ band is formed in α-Pu. The NTE mechanism at high T is g-SmS-like, whereas the PTE mechanism at low T is Ce-like. Dotted lines in (c) and (f) represent normal thermal expansions of $V(T)$ without the electronic contributions.

not change much in the $\gamma \rightarrow \alpha$ transition, i.e., being nearly trivalent (3+) for both γ and α-Ce [Fig. 4(b)] [61]. Then, the strong PTE in Ce is explained by the two-state Weiss model as shown in Fig. 4(c), which describes the volume collapse through the isostructural $\gamma \rightarrow \alpha$ transition.

IV. NTE AND PTE IN PU

Figure 2(e) indicates that Pu has diverse allotropic phases from the ground state of monoclinic α-Pu to bcc ϵ-Pu at the highest T. It also shows that, upon cooling, not only the volume jumps from ϵ-Pu to bct δ'-, and fcc δ-Pu but also the volume collapses from δ-Pu to γ-, β-, and α-Pu take place [47,48]. Among those, δ-Pu has the largest volume and shows the NTE feature.

Since the f-electron configuration in Pu is supposed to be the same as that in Sm compounds, the NTE mechanism in Pu at high T would be the same as that in g-SmS. But the extra existence of the PTE in Pu suggests that there would be some other mechanism in addition to the valence transition. We think that, at low T, the f-band bonding effect is operative in Pu as in the case of Ce. Namely, upon cooling from high T, there occurs first a valence transition between the near-trivalent (III) state of ϵ-Pu and the MV states of δ'- and δ-Pu ($n_f \approx 5.3$), resulting in the larger-volume phase of δ-Pu [62,63]. With further cooling, the dynamical charge fluctuation becomes almost frozen, and $5f$ electrons become delocalized via coherent f-band formation, resulting in the smaller-volume phase of α-Pu [64,65].

This mechanism is described schematically in Figs. 4(d)–4(f) by selecting three representative phases of Pu, α-, δ-, and ϵ-Pu. Note that $E(V)$ configurations for ϵ- and δ-Pu are similar to those for g-SmS [Fig. 3(a)] exhibiting the NTE, whereas $E(V)$ configurations for δ- and α-Pu are similar to those for γ- and α-Ce [Fig. 4(a)] exhibiting the PTE. Hence, the NTE mechanism between ϵ- and δ-Pu at high T would be

g-SmS-like, wherease the strong PTE mechanism between δ- and α-Pu at low T would be Ce-like.

V. NTE IN TOPOLOGICAL KONDO INSULATORS

Using the thermodynamic relation,

$$\left(\frac{\partial V}{\partial T}\right)_P = -\frac{(\partial P/\partial T)_V}{(\partial P/\partial V)_T}, \tag{2}$$

the thermal-expansion coefficient α_V is given by

$$\alpha_V = \frac{1}{V}\left(\frac{\partial V}{\partial T}\right)_P = \frac{1}{B}\left(\frac{\partial P}{\partial T}\right)_V, \tag{3}$$

where B is the bulk modulus, $B = -V(\frac{\partial P}{\partial V})_T$. Accordingly, α_V can be negative, provided $\frac{dP}{dT} < 0$ in the pressure-temperature (PT) phase diagram. In fact, all the above NTE systems given in Table I exhibit such characteristics in their (PT) phase diagrams.

In this respect, it is noteworthy that SmB_6, which was proposed to be a TKI, possesses an additional phase equilibrium line with $\frac{dP}{dT} < 0$ in its (PT) phase diagram at low T as shown in Fig. 5(a) [66]. SmB_6 is expected to become a TKI below T^*. $T^*(P)$ was determined from the resistivity $\rho(T)$ under pressure at which the increase in $\rho(T)$ after the final upturn slowed down noticeably. At T^*, the $4f$ band is anticipated to become fully coherent so as to form the Fermi liquid with the hybridization gap, inside which the topological surface states emerge [67]. This behavior of $\frac{dP}{dT} < 0$ suggests that the extra NTE feature would appear again near $T^* \sim 4$ K as depicted in Fig. 5(b), in addition to the observed NTE feature in the high-T regime where the minimum of α_V was located at $T \approx 50$ K [24].

In general, pressure tends to reduce the coherence of f electrons in Sm compounds [68], and so, under pressure, fully coherent f bands are to be formed at a lower T, which gives rise to $\frac{dT^*}{dP} < 0$. We think that this is the reason why $\frac{dP}{dT^*} < 0$ is
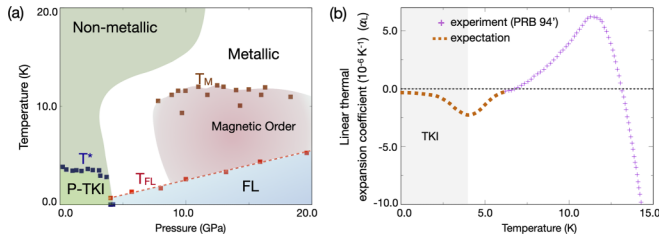
FIG. 5. (a) (P, T) phase diagram of SmB$_6$. Below T^*, TKI phase is expected to be stabilized. It is notable that $\frac{\partial P}{\partial T} < 0$ along T^*. Adapted from Ref. [66]. (b) Linear thermal-expansion coefficient α_L for SmB$_6$ was measured down to 5 K [24]. It is predicted that α_L becomes negative again in the TKI phase below 4 K as denoted by "expectation".

FIG. 6. (a) Interionic potential energy in solids. Due to the inherent anharmonicity, the interionic distance increases with increasing temperature (T) so as to exhibit normal PTE [5]. (b) Phonon origin of the NTE: Transverse-phonon mode and rigid-unit mode [1].

obtained in Fig. 5(a). In fact, the behavior of $\frac{dP}{dT^*} < 0$ implies the negative electronic Grüneisen parameter ($\gamma_G^e = -\frac{\partial \ln k_B T^*}{\partial \ln V}$) so that the NTE is supposed to be realized naturally.

SmS also has a similar behavior in its (PT) phase diagram, even though g-SmS would be a topological Kondo semimetal [54]. It was reported that there is a T' scale, which behaves just like T^* in SmB$_6$ [28]. Namely, in SmS too, the behavior of $\frac{dP}{dT} < 0$ along this phase equilibrium line indicates that there would be an additional NTE regime near T' ($\sim$3.7 K) besides that in the high-T regime where the minimum of α_V was observed at $T \approx 23$ K, which was considered to be T_{coh} of g-SmS [28,54].

To our knowledge, there are no thermal expansion data available for SmB$_6$ and g-SmS in such a very low-T regime. Furthermore, for the other well-studied TKI system, YbB$_{12}$, even the (PT) phase-diagram study has not been reported yet. Therefore, it would be very worthwhile to explore the thermal expansion properties of the TKI candidates of SmB$_6$, g-SmS, and YbB$_{12}$ more carefully in the low-T regime.

VI. FINAL REMARKS AND CONCLUSION

We have argued that the anomalous thermal expansion behaviors in various f-electron MV systems have the electronic origin. Note that the f-electron MV systems are expected to have strong electron-phonon (e-ph) interaction, which would produce the renormalized electronic spectra as well as the renormalized phonon frequencies. Therefore, there would be some amount of contribution from the e-ph interaction to the thermal expansion in addition to the bare f-electronic contributions (i.e., valence transition and coherence physics considered in the present paper). In fact, the effects of the e-ph interaction on the thermal expansion in f-electron systems have been examined previously [69–71]. Furthermore, the effects of the e-ph interaction on the thermal expansion has been theoretically investigated based on the two-state Weiss model, which was employed in the present paper [17].

According to previous reports, there are indeed non-negligible contributions from the e-ph interaction. However, for the physical e-ph interaction parameters of real systems, the overall behavior of T-dependent NTE is more or less similar to the case without considering the e-ph interaction. Only the quantitative values, such as the minimum positions of $V(T)$ and $\alpha_V(T)$, are changed a little bit [71]. In the present
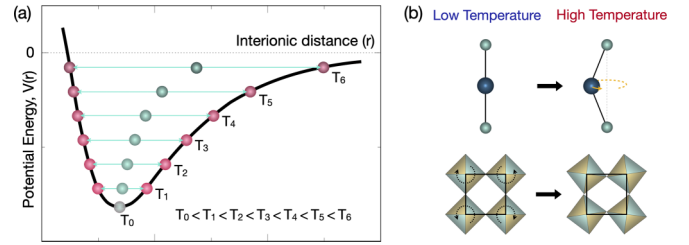
paper, we have tried to understand the NTE observed in the (Sm, Yb)-based MV systems in comparison with the PTE observed in the (Ce, Eu)-based MV systems, employing the phenomenological theory of the two-state Weiss model. In this context, the analyses of the present paper, albeit rather qualitative, will suffice to understand the underlying NTE and PTE physics observed in the f-electron MV systems.

We have identified that the NTE phenomena observed in Sm- and Yb-based MV systems originate from the T-induced valence transitions from the near-trivalent to the MV (near-divalent) state. We have discussed the different role of valence transitions in the thermal expansion between (Sm, Yb)-based MV systems and their electron-hole symmetric counterparts, (Ce, Eu)-based MV systems. Our finding for the MV systems is that the NTE would be realized when their excited states have smaller volumes as in (Sm, Yb) compounds, whereas the PTE would be realized when their excited states have larger volumes as in (Ce, Eu) compounds. We have explained the intriguing thermal expansion behavior of Pu, i.e,, the appearance of both the NTE and the PTE features in series with decreasing T, in terms of the g-SmS-like valence transition first and then the Ce-like coherent f-band formation. Finally, based on the (PT) phase diagram, we have predicted the possible existence of an additional NTE feature in SmB$_6$, g-SmS, and YbB$_{12}$ in the low-T regime where the TKI phases are expected to be stabilized.

The present paper demonstrates that the thermal expansion measurement, albeit conventional and rather simple,
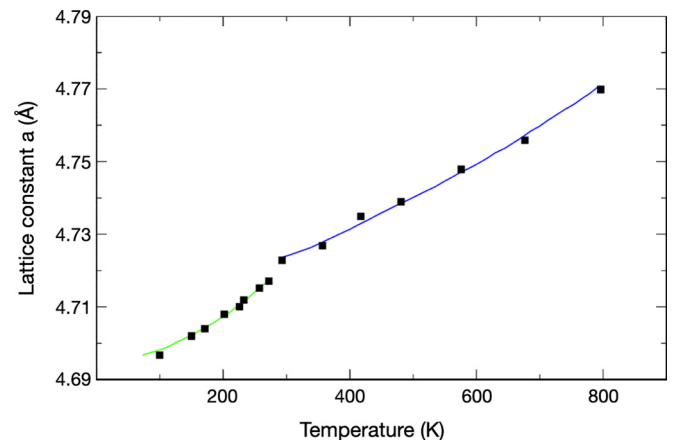

FIG. 7. PTE of a Ce-based MV system, CeSn$_3$ ($T_{VT} \approx 260$ K). Data adapted from Ref. [59].

can be utilized as an important tool in understanding the complicated physics and hidden peculiarities manifested in strongly correlated *f*-electron systems. Therefore, in order to unravel intriguing physics of strongly correlated *f*-electron systems, such as physics of the TKI, more careful low-*T* thermal-expansion measurements as well as more quantitative theoretical studies are urgently required.

ACKNOWLEDGMENTS

APPENDIX

Figure 6(a) shows a typical anharmonic interionic-potential energy in solids, which yields the normal PTE, and Fig. 6(b) provides examples of transverse phonon mode and rigid-unit mode, which yield the NTE of phonon origin.

Figure 7 shows the PTE of a Ce-based MV system $CeSn_3$.

[1] J. S. O. Evans, T. A. Mary, and A. W. Sleight, Physica B **241-243**, 311 (1997).

[2] T. H. K. Barron and G. K. White, *Heat Capacity and Thermal Expansion at Low Temperatures*, the International Cryogenics Monograph Series (Springer, New York, 1999).

[3] G. D. Barrera, J. A. O. Bruno, T. H. K. Barron, and N. L. Allan, J. Phys.: Condens. Matter **17**, R217(R) (2005).

[4] W. Miller, C. W. Smith, D. S. Mackenzie, and K. E. Evans, J. Mater. Sci. **44**, 5441 (2009).

[5] J. Chen, L. Hu, J. Deng, and X. Xing, Chem. Soc. Rev. **44**, 3522 (2015).

[6] M. T. Dove and H. Fang, Rep. Prog. Phys. **79**, 066503 (2016).

[7] Z.-K. Liu, S.-L. Shang, and Y. Wang, Materials **10**, 410 (2017).

[8] K. Takenaka, Front. Chem. **6**, 267 (2018).

[9] J. P. Attfield, Front. Chem. **6**, 371 (2018).

[10] E. Liang, Q. Sun, H. Yuan, J. Wang, G. Zeng, and Q. Gao, Front. Phys. **16**, 53302 (2021).

[11] G. K. White, J. Phys. D: Appl. Phys. **6**, 2070 (1973).

[12] M. Hortal and A. J. Leadbetter, J. Phys. C: Solid State Phys. **5**, 2129 (1972).

[13] T. A. Mary, J. S. O. Evans, T. Vogt, and A. W. Sleight, Science **272**, 90 (1996).

[14] C. E. Guillaume, C. R. Acad. Sci. **125**, 235 (1897).

[15] R. J. Weiss, Proc. Phys. Soc., London **82**, 281 (1963).

[16] V. L. Moruzzi, Phys. Rev. B **41**, 6939 (1990).

[17] D. I. Khomskii and F. V. Kusmartsev, Phys. Rev. B **70**, 012413 (2004).

[18] M. Lang, R. Schefzyk, F. Steglich, and N. Grewe, J. Magn. Magn. Mater. **63-64**, 79 (1987).

[19] K. Andres, J. E. Graebner, and H. R. Ott, Phys. Rev. Lett. **35**, 1779 (1975).

[20] V. V. Novikov, N. V. Mitroshenkov, A. V. Matovnikov, B. I. Kornev, and V. B. Koltsov, Physica B **506**, 152 (2017).

[21] R. Schefzyk, M. Peschke, F. Steglich, and K. Winzer, J. Magn. Magn. Mater. **63-64**, 67 (1987).

[22] A. de Visser, K. Bakker, and J. Pierre, Physica B **186-188**, 577 (1993).

[23] V. A. Trounov, A. L. Malyshev, D. Yu Chernyshov, M. M. Korsukova, V. N. Gurin, L. A. Aslanov, V. V. Chernyshev, J. Phys.: Condens. Matter **5**, 2479 (1993).

[24] D. Mandrus, J. L. Sarrao, A. Lacerda, A. Migliori, J. D. Thompson, and Z. Fisk, Phys. Rev. B **49**, 16809 (1994).

[25] N. N. Sirota, V. V. Novikov, V. A. Vinokurov, Y. B. Paderno, Phys. Solid State **40**, 1856 (1998).

[26] J. Arvanitidis, K. Papagelis, S. Margadonna, K. Prassides, and A. N. Fitch, Nature (London) **425**, 599 (2003).

[27] K. Iwasa, T. Tokuyama, M. Kohgi, N. K. Sato, and N. Mori, Physica B **359-361**, 148 (2005).

[28] K. Imura, K. Matsubayashi, H. S. Suzuki, K. Deguchi, and N. K. Sato, Physica B **404**, 3028 (2009).

[29] D. Asai, Y. Mizuno, H. Hasegawa, Y. Yokoyama, Y. Okamoto, N. Katayama, H. S. Suzuki, Y. Imanaka, and K. Takenaka, Appl. Phys. Lett. **114**, 141902 (2019).

[30] K. Takenaka, D. Asai, R. Kaizu, Y. Mizuno, Y. Yokoyama, Y. Okamoto, N. Katayama, H. S. Suzuki, and Y. Imanaka, Sci. Rep. **9**, 122 (2019).

[31] D. G. Mazzone, M. Dzero, A. M. M. Abeykoon, H. Yamaoka, H. Ishii, N. Hiraoka, J.-P. Rueff, J. M. Ablett, K. Imura, H. S. Suzuki, J. N. Hancock, and I. Jarrige, Phys. Rev. Lett. **124**, 125701 (2020).

[32] S. L. Bud'ko, J. C. Frederick, E. D. Mun, P. C. Canfield, and G. M. Schmiedeshoff, J. Phys.: Condens. Matter **20**, 025220 (2008).

[33] M. Kasaya, F. Iga, M. Takigawa, and T. Kasuya, J. Magn. Magn. Mater. **47-48**, 429 (1985).

[34] V. V. Novikov, N. A. Zhemoedov, A. V. Matovnikov, N. V. Mitroshenkov, E. A. Popova, A. K. Tolstosheev, B. Z. Malkin, and S. L. Budko, Phys. Rev. Mater. **2**, 054401 (2018).

[35] S. Margadonna, J. Arvanitidis, K. Papagelis, and K. Prassides, Chem. Mater. **17**, 4474 (2005).

[36] W. C. M. Mattens, H. Hoelscher, G. J. M. Tuin, A. C. Moleman, and F. R. de Boer, J. Magn. Magn. Mater. **15-18**, 982 (1980).

[37] R. Pott, R. Schefzyk, D. Wohlleben, and A. Junod, Z. Phys. B: Condens. Matter **44**, 17 (1981).

[38] H. Yamaoka, N. Tsujii, Y. Utsumi, H. Sato, I. Jarrige, Y. Yamamoto, J.-F. Lin, N. Hiraoka, H. Ishii, K.-D. Tsuei, and J. Mizuki, Phys. Rev. B **87**, 205120 (2013).

[39] Y. Uwatoko, G. Oomi, J. D. Thompson, P. C. Canfield, and Z. Fisk, Physica B **186-188**, 593 (1993).

[40] R. Hauser, T. Ishii, Y. Uwatoko, G. Oomi, E. Bauer, and E. Gratz, J. Magn. Magn. Mater. **157-158**, 679 (1996).

[41] R. Pott, *Thermal Expansion and Specific Heat of Mixed Valence Compounds in Physics and Chemistry of Electrons and Ions in Condensed Matter*, edited by J. V. Acrivos, N. F. Mott, and A. D. Yoffe, NATO ASI Series Vol. 130 (Springer, Dordrecht, 1984).

[42] B. Kindler, D. Finsterbusch, R. Graf, F. Ritter, W. Assmus, and B. Lüthi, Phys. Rev. B **50**, 704 (1994).

[43] Y.-F. Liao, B. T. Chiogo, T. Clausse, T. Mazet, K.-D. Tsuei, D. Malterre, and A. Chainani, Commun. Mater. **3**, 23 (2022).

[44] T. Takeuchi, S. Yoshiuchi, Y. Hirose, F. Honda, R. Settai, and Y. Onuki, JPS Conf. Proc. **3**, 011017 (2014).

[45] R. Takke, M. Niksch, W. Assmus, and B. Lüthi, Z. Phys. B: Condens. Matter **44**, 33 (1981).

[46] The investigation of the origin of Ce-based NTE systems will be presented elsewhere.

[47] E. Jette, J. Chem. Phys. **23**, 365 (1955).

[48] P. Söderlind, A. Landa, and B. Sadigh, Adv. Phys. **68**, 1 (2019), and references therein.

[49] M. Dzero, K. Sun, V. Galitski, and P. Coleman, Phys. Rev. Lett. **104**, 106408 (2010).

[50] H. Weng, J. Zhao, Z. Wang, Z. Fang, and X. Dai, Phys. Rev. Lett. **112**, 016403 (2014).

[51] C.-J. Kang, D.-C. Ryu, J. Kim, K. Kim, J.-S. Kang, J. D. Denlinger, G. Kotliar, and B. I. Min, Phys. Rev. Mater. **3**, 081201(R) (2019).

[52] C.-J. Kang, K. Kim, and B. I. Min, J. Phys.: Condens. Matter **34**, 271501 (2022), and reference therein.

[53] Z.-K. Liu, Y. Wang, and S. Shang, Sci. Rep. **4**, 7043 (2014).

[54] C.-J. Kang, H. C. Choi, K. Kim, and B. I. Min, Phys. Rev. Lett. **114**, 166404 (2015).

[55] E. Müller-Hartmann, Solid State Commun. **31**, 113 (1979).

[56] E. V. Sampathkumaran, L. C. Gupta, R. Vijayaraghavan, K. V. Gopalakrishnan, R. G. Pillay, and H. G. Devare, J. Phys. C: Solid State Phys. **14**, L237 (1981).

[57] Y. Ōnuki, M. Hedo, and F. Honda, J. Phys. Soc. Jpn. **89**, 102001 (2020).

[58] B. Wolf, F. Spathelf, J. Zimmermann, T. Lundbeck, M. Peters, K. Kliemt, C. Krellner, and M. Lang, arXiv:2210.12227.

[59] G. A. Costa, F. Canepa, and G. L. Olcese, Solid State Commun. **44**, 67 (1982).

[60] X.-G. Zhu, Y. Liu, Y.-W. Zhao, Y.-C. Wang, Y. Zhang, C. Lu, Y. Duan, D.-H. Xie, W. Feng, D. Jian, Y.-H. Wang, S.-Y. Tan, Q. Liu, W. Zhang, Y. Liu, L.-Z. Luo, X.-B. Luo, Q.-Y. Chen, H.-F. Song, and X.-C. Lai, npj Quantum Mater. **5**, 47 (2020).

[61] J. Kim, D.-C. Ryu, C.-J. Kang, K. Kim, H. Choi, T.-S. Nam, and B. I. Min, Phys. Rev. B **100**, 195138 (2019).

[62] T. Lee, M. I. Baskes, A. C. Lawson, S. P. Chen, and S. M. Valone, Materials **5**, 1040 (2012).

[63] N. Harrison, J. B. Betts, M. R. Wartenbe, F. F. Balakirev, S. Richmond, M. Jaime, and P. H. Tobash, Nat. Commun. **10**, 3159 (2019).

[64] S. Y. Savrasov, G. Kotliar, and E. Abrahams, Nature (London) **410**, 793 (2001).

[65] J. H. Shim, K. Haule, and G. Kotliar, Nature (London) **446**, 513 (2007).

[66] Y. Zhou, Q. Wu, P. F. S. Rosa, R. Yu, J. Guo, W. Yi, S. Zhang, Z. Wang, H. Wang, S. Cai, K. Yang, A. Li, Z. Jiang, S. Zhang, X. Wei, Y. Huang, P. Sun, Y.-f. Yang, Z. Fisk, Q. Si, Z. Zhao *et al.*, Sci. Bull. **62**, 1439 (2017).

[67] J. Kim, K. Kim, C.-J. Kang, S. Kim, H. C. Choi, J.-S. Kang, J. D. Denlinger, and B. I. Min, Phys. Rev. B **90**, 075131 (2014).

[68] S. Doniach, Physica B+C **91**, 231 (1977); Note that pressure effects in the Doniach phase diagram are just opposite between (Sm, Yb) and (Ce, Eu) compounds.

[69] P. Entel and N. Grewe, Z. Phys. B: Condens. Matter **34**, 229 (1979).

[70] M. Rivas, J. Rössler, and M. Kiwi, Phys. Rev. B **43**, 3593 (1991).

[71] E. V. Nefeodova, P. A. Alekseev, V. N. Lazukov, and I. P. Sadikov, Physica B **312-313**, 376 (2002).